Article

SOURCE DATA | TRANSPARENT PROCESS | OPEN ACCESS

THE EMBO JOURNAL

Infection and transmission of SARS-CoV-2 depend on heparan sulfate proteoglycans

Marta Bermejo-Jambrina[1,†], Julia Eder[1,†], Tanja M Kaptein[1], John L vanHamme[1], Leanne C Helgers[1], Killian E Vlaming[1], Philip J M Brouwer[2], Ad C vanNuenen[1], Marcel Spaargaren[3], Godelieve J deBree[4], Bernadien M Nijmeijer[1], Neeltje A Kootstra[1], Marit J vanGils[2], Rogier W Sanders[2,5] & Teunis B H Geijtenbeek[1,*]

Abstract

The current pandemic caused by severe acute respiratory syndrome coronavirus 2 (SARS-CoV-2) and outbreaks of new variants highlight the need for preventive treatments. Here, we identified heparan sulfate proteoglycans as attachment receptors for SARS-CoV-2. Notably, neutralizing antibodies against SARS-CoV-2 isolated from COVID-19 patients interfered with SARS-CoV-2 binding to heparan sulfate proteoglycans, which might be an additional mechanism of antibodies to neutralize infection. SARS-CoV-2 binding to and infection of epithelial cells was blocked by low molecular weight heparins (LMWH). Although dendritic cells (DCs) and mucosal Langerhans cells (LCs) were not infected by SARS-CoV-2, both DC subsets efficiently captured SARS-CoV-2 via heparan sulfate proteoglycans and transmitted the virus to ACE2-positive cells. Notably, human primary nasal cells were infected by SARS-CoV-2, and infection was blocked by pre-treatment with LMWH. These data strongly suggest that heparan sulfate proteoglycans are important attachment receptors facilitating infection and transmission, and support the use of LMWH as prophylaxis against SARS-CoV-2 infection.

Keywords dendritic cells; epithelial cells; Heparan sulfate proteoglycans; low molecular weight heparins; SARS-CoV-2

Subject Category Microbiology, Virology & Host Pathogen Interaction

DOI 10.15252/embj.2020106765 | Received 10 September 2020 | Revised 1 September 2021 | Accepted 2 September 2021 | Published online 23 September 2021

The EMBO Journal (2021) 40: e106765

Introduction

Severe acute respiratory syndrome coronavirus 2 (SARS-CoV-2) emerged in Wuhan, China, in late 2019 and can cause coronavirus disease 2019 (COVID-19), an influenza-like disease ranging from mild respiratory symptoms to severe lung injury, multiorgan failure, and death (Yuki *et al*, 2020; Zhou *et al*, 2020; Zhu *et al*, 2020). SARS-CoV-2 spread quickly and has caused a pandemic with a severe impact on global health and world economy (Nicola *et al*, 2020; World Health Organization, 2020b). SARS-CoV-2 is transmitted predominantly via large droplets expelled from the upper respiratory tract through sneezing and coughing (Ferioli *et al*, 2020; Harapan *et al*, 2020) and is subsequently taken up via mucosal surfaces of the nose, mouth, and eyes (Peiris *et al*, 2003). SARS-CoV-2 infects epithelial cells in the respiratory tract, such as ciliated mucus-secreting bronchial epithelial cells and type 1 pneumocytes in the lung, as well as epithelial cells in the gastrointestinal tract (Hui *et al*, 2020; Lamers *et al*, 2020). For more than a year, lockdown strategies and social distancing have been used to mitigate viral spread but due to negative socioeconomic consequences these are not feasible long-term solutions (Brooks *et al*, 2020; Wright *et al*, 2020). Currently, several COVID-19 vaccines have been developed and worldwide vaccination programs have been initiated (Mathieu *et al*, 2021), which aim to curb and stop the pandemic. However, immunocompromised individuals as well as people on immunosuppressive drugs are potentially less protected by vaccinations (preprint: Agha *et al*, 2021; Boyarsky *et al*, 2021). Moreover, current vaccine candidates might be less effective against new SARS-CoV-2 variants (Collier *et al*, 2021; Wang *et al*, 2021). Thus, there is a need for protective strategies specifically targeting SARS-CoV-2 to prevent further dissemination.

1 Department of Experimental Immunology, Amsterdam institute for Infection and Immunity, Amsterdam University Medical Centers, University of Amsterdam, Amsterdam, The Netherlands
2 Department of Medical Microbiology, Amsterdam institute for Infection and Immunity, Amsterdam University Medical Centers, University of Amsterdam, Amsterdam, The Netherlands
3 Department of Pathology, Lymphoma and Myeloma Center Amsterdam (LYMMCARE), Cancer Center Amsterdam (CCA), Amsterdam University Medical Centers, University of Amsterdam, Amsterdam, The Netherlands
4 Department of Internal Medicine, Amsterdam institute for Infection and Immunity, Amsterdam University Medical Centers, University of Amsterdam, Amsterdam, The Netherlands
5 Department of Microbiology and Immunology, Weill Medical College of Cornell University, New York, NY, USA
*Corresponding author. Tel: +31 20 566 8590; E-mail: t.b.geijtenbeek@amsterdamumc.nl
†These authors contributed equally to this work

SARS-CoV-2 belongs to the betacoronaviruses, a family that also includes SARS-CoV and MERS-CoV (Letko *et al*, 2020). The coronavirus Spike (S) protein is a class I fusion protein that mediates virus entry (Bosch *et al*, 2003; Hulswit *et al*, 2016). The S protein consists of two subunits: S1 directly engages via its receptor-binding domain (RBD) with host surface receptors (Li *et al*, 2005; Wang *et al*, 2013) and S2 mediates fusion between virus and cell membrane (Burkard *et al*, 2014; Xia *et al*, 2020).

SARS-CoV-2 uses angiotensin-converting enzyme 2 (ACE2) as its main receptor (Hoffmann *et al*, 2020; Letko *et al*, 2020). ACE2 is a type I integral membrane protein abundantly expressed on epithelial cells lining the respiratory tract (Hamming *et al*, 2004) but also the ileum, esophagus, and liver (Zou *et al*, 2020b) and ACE2 expression dictates SARS-CoV-2 tropism (Lamers *et al*, 2020). However, it remains unclear whether SARS-CoV-2 requires other receptors for virus entry. Neutralizing monoclonal antibodies against SARS-CoV-2 have been identified that are directed not only at the RBD but also outside the RBD (Brouwer *et al*, 2020), suggesting that other mechanisms of neutralization or other (co-) receptors might be involved.

Heparan sulfates are expressed by most cells, including epithelial cells, as heparan sulfate proteoglycans and these have been shown to interact with viruses such as HIV-1, HCV, Sindbis virus, and also SARS-CoV (Roderiquez *et al*, 1995; Byrnes & Griffin, 1998; Jiang *et al*, 2012; Milewska *et al*, 2014; Nijmeijer *et al*, 2020). Recently, it was shown that the S protein of SARS-CoV-2 interacts with heparan sulfates, which might be required for infection (Clausen *et al*, 2020; Zhang *et al*, 2020).

Here, we show that heparan sulfate proteoglycans are important for infection of polarized epithelial cells as well as primary nasal cells with SARS-CoV-2. Infection is inhibited by heparin and low molecular weight heparins (LMWH). Mucosal dendritic cell subsets captured SARS-CoV-2 via heparan sulfate proteoglycans. The different DC subsets did not become infected but transmitted SARS-CoV-2 to ACE2-positive cells, which might facilitate virus dissemination. Our findings suggest that heparan sulfate proteoglycans function as attachment receptors for SARS-CoV-2 and LMWH can be used as prophylactics against SARS-CoV-2 or prevent dissemination early after infection.

Results

SARS-CoV-2 pseudovirus binds to heparan sulfates expressed by cells

We incubated Huh7.5 cells that express ACE2 (Fig EV1A) with SARS-CoV-2 pseudovirus, which consists of HIV-1 particles pseudotyped with SARS-CoV-2 S protein (Brouwer *et al*, 2020). Virus binding was determined by measuring HIV-1 p24 binding by ELISA. SARS-CoV-2 pseudovirus attached to Huh7.5 cells, which was blocked by anti-ACE2 antibodies (anti-ACE2) as well as by neutralizing antibodies from COVID-19 patients (Brouwer *et al*, 2020) (Fig 1A). Unfractionated (UF) heparin inhibited binding of SARS-CoV-2 pseudovirus to Huh7.5 cells comparable to the neutralizing or anti-ACE2 antibodies (Fig 1A). Enzymatic removal of heparan sulfates on the cell surface by heparinase treatment decreased SARS-CoV-2 virus binding (Figs 1B and EV1B). Exostosin-1 (EXT1) knockdown decreased expression of heparan sulfates on the cell surface (Ren *et al*, 2018) (Fig 1C). SARS-CoV-2 pseudovirus attached to XG1 cells, which was blocked by UF heparin, whereas knockdown of EXT1 abrogated SARS-CoV-2 pseudovirus binding (Fig 1D). These data suggest that heparan sulfates are important for attachment of SARS-CoV-2 to cells.

Low molecular weight heparins inhibit SARS-CoV-2 infection

To determine the effect of UF heparin on SARS-CoV-2 infection, we infected Huh7.5 cells with SARS-CoV-2 pseudovirus, expressing the luciferase reporter gene, and determined infection by measuring luciferase reporter activity. UF heparin blocked infection in a dose-dependent manner (Fig 2A). Low molecular weight heparin (LMWH) have replaced UF heparin in the clinic as anti-coagulant treatment due to their smaller size and superior pharmacological properties (Kakkar, 2004). LMWH enoxaparin blocked SARS-CoV-2 pseudovirus infection in a dose-dependent manner to similar levels as UF heparin (Fig 2A) without affecting cell viability of Huh7.5 cells (Fig EV1C). Not only enoxaparin but also other clinically approved LMWH blocked binding of SARS-CoV-2 pseudovirus to Huh7.5 cells (Fig 2B). The different LMWH also blocked infection of Huh7.5 cells with SARS-CoV-2 pseudovirus to a similar extent as enoxaparin (Fig 2C).

Next, we investigated whether ACE2 is required for infection in presence of heparan sulfates. Human kidney epithelial 293T cells were not susceptible to SARS-CoV-2 pseudovirus whereas ectopic expression of ACE2 rendered these cells susceptible to SARS-CoV-2 pseudovirus (Figs 2D and EV1D and E). Infection was abrogated by both LMWH enoxaparin and UF heparin to a similar level as antibodies against ACE2 (Fig 2D). The combination of ACE2 antibodies and LMWH enoxaparin or UF heparin blocked infection of 293T-ACE2 cells (Fig 2D). These data suggest that heparan sulfates act as attachment receptors that allow the virus to bind to cells, facilitating infection via ACE2. Next, we investigated whether pre-incubation of SARS-CoV-2 with LWMH prevents ACE2 binding. The primary SARS-CoV-2 isolate (hCoV-19/Italy) interacted with immobilized ACE2 and, notably, pre-treatment of the virus with LMWH did not affect ACE2 binding (Fig EV1F). These data suggest that LMWH prevent virus attachment but do not affect the interaction with ACE2.

Simian Vero E6 cells are highly susceptible to SARS-CoV-2, which causes severe cytopathic effects (CPE) (Zhou *et al*, 2020), and therefore, we investigated the role of LMWH upon SARS-CoV-2 infection by measuring the cytopathic effects. Infection of VeroE6 with a primary SARS-CoV-2 isolate (hCoV-19/Italy) caused severe CPE as cell viability decreased (Fig 2E), which was counteracted by LMWH enoxaparin in a concentration-dependent manner. These data support an important role for heparan sulfates in ACE2-dependent infection of cells with SARS-CoV-2.

SARS-CoV-2 infection of polarized epithelial cells is blocked by UF heparin and LMWH

The colorectal adenocarcinoma Caco-2 and bronchial adenocarcinoma Calu-3 cells represent models for human intestinal and respiratory epithelial cells, respectively (Artursson *et al*, 2001; Harcourt *et al*, 2011). Both cell lines were cultured on microporous filters

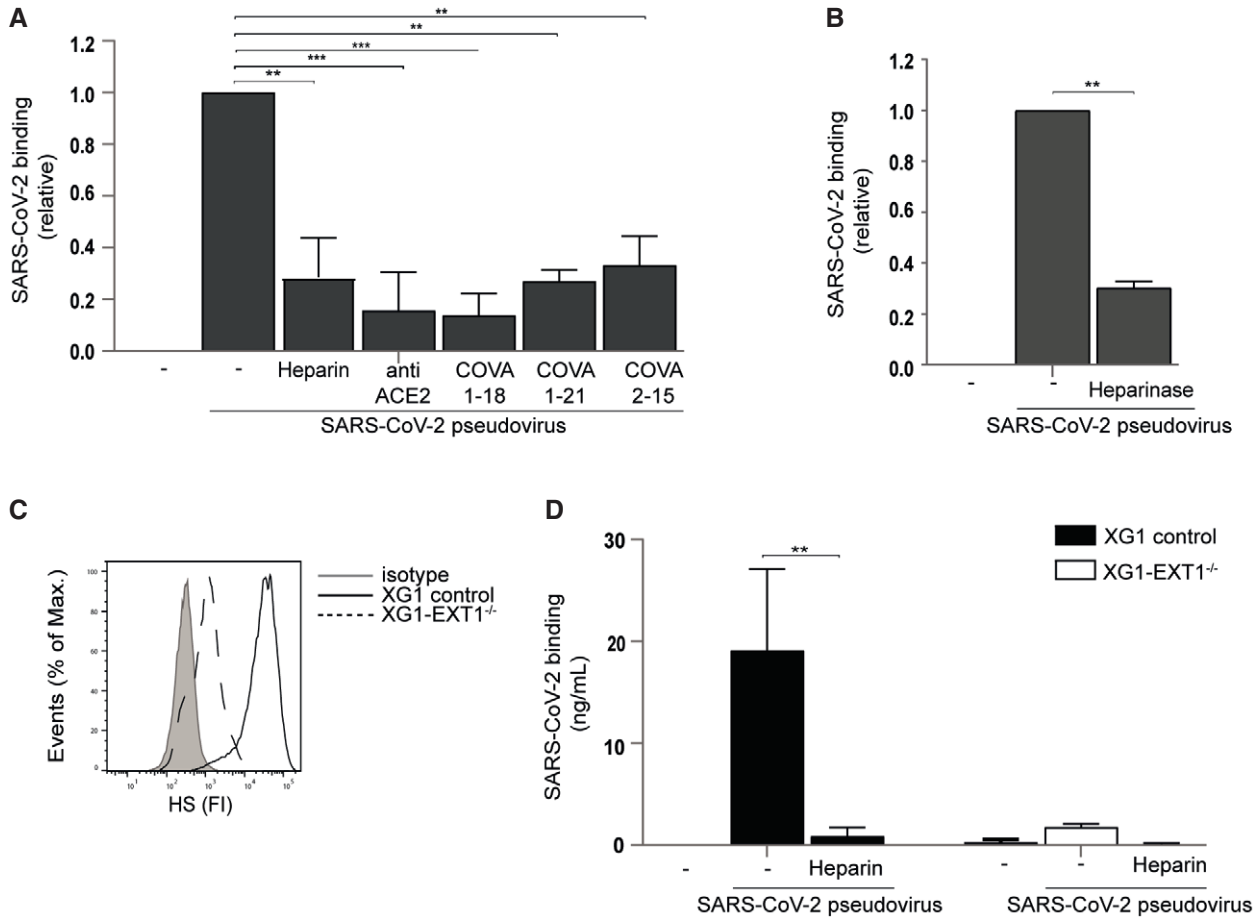

Figure 1. SARS-CoV-2 pseudovirus binds to heparan sulfates.

A Huh7.5 cells were pre-incubated with neutralizing antibody to ACE2 and SARS-CoV-2 pseudovirus was pre-incubated with patient isolated mAb COVA1-18, COVA1-21 and COVA2-15 (10 μg/ml) or UF heparin (250 IU/ml) for 30 min at 37°C. SARS-CoV-2 pseudovirus alone or with blocks was added to the cells for 4 h at 4°C and binding was determined by ELISA.

B Heparan sulfates were removed from Huh7.5 cells by enzymatic treatment with heparinase III for 1 h at 37°C, then washed, and exposed to SARS-CoV-2 pseudovirus for 4 h at 4°C. Treated and untreated cells were subsequently lysed and binding was determined by ELISA.

C Flow cytometry analysis of cell surface expression of heparan sulfates (HS) in control transduced cells or upon CRISPR/Cas9-mediated EXT1 KO (EXT1$^{-/-}$).

D Control and EXT1$^{-/-}$ XG1 cells were exposed to SARS-CoV-2 pseudovirus or SARS-CoV-2 pseudovirus pre-treated with 250 IU/ml UF heparin for 30 min at 37°C. After incubation for 4 h at 4°C, cells were lysed and binding was measured by ELISA.

Data information: Data show the mean values and error bars are the SEM. Statistical analysis was performed using (A) ordinary one-way ANOVA with Tukey multiple-comparison test. *$P \leq 0.05$, **$P \leq 0.01$, ***$P \leq 0.001$ ($n = 3$), (B) unpaired Student's t-test with Welch's correction. *$P \leq 0.05$, **$P \leq 0.01$ ($n = 3$), (D) two-way ANOVA with Dunnett's multiple-comparison test. *$P \leq 0.05$, **$P \leq 0.01$ ($n = 3$).

with an air–liquid interface to achieve a polarized monolayer and polarization was monitored by transepithelial electrical resistance (TEER). TEER increased over time to confirm that the cells are polarized after culture of more than 14 days (Fig 3A). Undifferentiated Caco-2 and Calu-3 expressed low levels of ACE2 but polarization of the cells highly increased ACE2 expression (Fig 3B). SARS-CoV-2 pseudovirus bound to both polarized Caco-2 and Calu-3 cells and binding was significantly blocked by LMWH to similar levels as antibodies against ACE2 (Fig 3C and D). The combination of an antibody against ACE2 and LMWH enoxaparin did not further decrease binding. We next infected polarized Calu-3 cells with the primary SARS-CoV-2 isolate for 24 h, washed, and after another 24 h determined productive infection. Infection was determined by measuring SARS-CoV-2 ORF1b transcripts present during infection in cells but also in virus particles. Calu-3-polarized cells were productively infected by the SARS-CoV-2 isolate as shown by the SARS-CoV-2 ORF1b viral transcripts in the cell lysates, and the secretion of SARS-CoV-2 virus particles in the supernatant (Fig 3E and F as well as EV3A and EV3B). Cell viability was not affected by infection as checked by GAPDH expression. Notably, productive infection of Calu-3 cells was inhibited by LMWH to a similar level as ACE2 antibodies (Figs 3E and F as well as EV3A and B). These data suggest that heparan sulfates are required for binding and infection of polarized respiratory epithelial cells with SARS-CoV-2 pseudovirus as well as primary SARS-CoV-2 isolate.

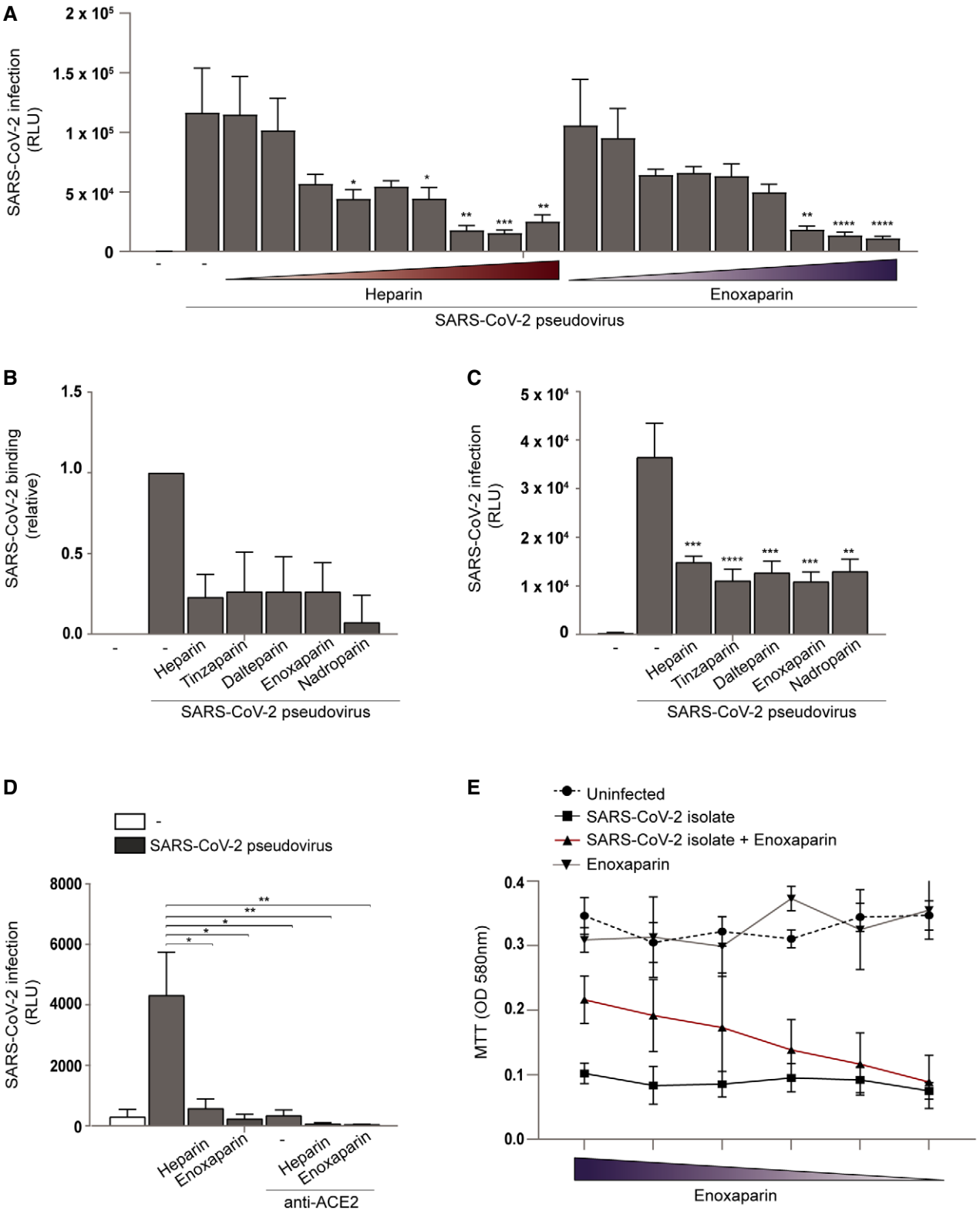

Figure 2.

Figure 2. Low molecular weight heparins inhibit SARS-CoV-2 infection.

A Huh7.5 cells were exposed to SARS-CoV-2 pseudovirus directly or after pre-treatment with different concentrations (0.0001, 0.001, 0.1, 0.5, 1, 5, 50, 100, 250 IU/ml) of UF heparin or LMWH enoxaparin for 30 min at 37°C. Infection was determined by luciferase reporter activity after 5 days.

B SARS-CoV-2 pseudovirus was pre-incubated for 30 min at 37°C with UF heparin (250 IU/ml) or LMWH tinzaparin (250 IU/ml) or dalteparin (250 IU/ml) or enoxaparin (250 IU/ml) or nadroparin (250 IU/ml). Huh7.5 was exposed to the SARS-CoV-2 pseudovirus, alone or treated with different LMWH for 4 h at 4°C, washed, lysed and binding was determined by ELISA.

C SARS-CoV-2 pseudovirus was pre-incubated for 30 min at 37°C with UF heparin (250 IU/ml) or LMWH tinzaparin (250 IU/ml) or dalteparin (250 IU/ml) or enoxaparin (250 IU/ml) or nadroparin (250 IU/ml). Huh7.5 cells were infected with SARS-CoV-2 pseudovirus in presence or absence of different LMWH and infection was determined after 5 days by luciferase reporter activity.

D 293T cells expressing ACE2 were infected with SARS-CoV-2 pseudovirus in presence or absence of antibodies against ACE2, UF heparin (250 IU/ml), or LMWH enoxaparin (250 IU/ml), and infection was determined after 3 days by luciferase reporter activity.

E VeroE6 cells were infected with SARS-CoV-2 isolate (hCoV-19/Italy; 100 TCID/ml) previously treated with serial dilutions of LMWH enoxaparin. Cell viability was determined using an MTT assay (n = 3 donors measured in triplicate).

Data information: Data show the mean values and error bars are the SEM. Statistical analysis was performed using (A) ordinary one-way ANOVA with Dunnett's multiple-comparison test. *$P \leq 0.05$, **$P \leq 0.01$, ***$P \leq 0.001$, ****$P \leq 0.0001$ (n = 3 donors measured in triplicate). (B) Ordinary one-way ANOVA with Tukey's multiple-comparison test (n = 3 donors measured in monoplo), (C) ordinary one-way ANOVA with Dunnett's multiple-comparison test. *$P \leq 0.05$, **$P \leq 0.01$, ***$P \leq 0.001$, ****$P \leq 0.0001$ (n = 3 donors measured in triplicate), (D) ordinary one-way ANOVA with Dunnett's multiple-comparison test. *$P \leq 0.05$, **$P \leq 0.01$ (n = 3 measured in triplicate). RLU: relative light units.
Source data are available online for this figure.

Heparan sulfate proteoglycans Syndecan 1 and 4 are important for SARS-CoV-2 binding

The heparan sulfate proteoglycan family of Syndecans is particularly important in facilitating cell adhesion of several viruses (Bacsa *et al*, 2011; Nijmeijer *et al*, 2020). Therefore, we used the Namalwa B cell line that ectopically expressed Syndecan 1 or Syndecan 4 (Fig EV2A–C) as these Syndecans are expressed by epithelial cells (Hayashida *et al*, 2006; Teng *et al*, 2012). Namalwa cells did not express ACE2 (Fig EV1A). Syndecan 1 and Syndecan 4 expressing Namalwa cells bound more efficiently with SARS-CoV-2 pseudovirus than the parental Namalwa cells (Fig 4A). Both UF heparin and LMWH enoxaparin blocked the interaction of Syndecan 1- and 4-expressing cells with SARS-CoV-2 pseudovirus (Fig 4A). Moreover, Syndecan 1-expressing cells did not interact with control pseudovirus lacking the SARS-CoV-2 S protein neither did LMWH enoxaparin affect the interaction (Fig EV2D). Similarly, control pseudovirus did not interact with Huh7.5 cells (Fig EV2D). These data suggest that the interaction of Syndecans with SARS-CoV-2 is specific and depends on the S protein.

Next, we measured binding of primary SARS-CoV-2 to Syndecan expressing cells. The primary SARS-CoV-2 isolate attached to both Syndecan 1 and Syndecan 4 expressing cells and LMWH enoxaparin blocked binding to background levels similar to those observed for the parental control cells (Figs 4B and EV3B). Cell viability was unaffected as determined by GAPDH expression. These data indicate that Syndecan 1 and 4 are important heparan sulfate proteoglycans involved in SARS-CoV-2 binding and infection.

Neutralizing antibodies against SARS-CoV-2 interfere with SARS-CoV-2 binding to Syndecan 1

Several antibodies against SARS-CoV-2 were isolated from COVID-19 patients, and some of these were potent neutralizing antibodies against SARS-CoV-2 that target the RBD (COVA1-15, COVA1-18) as well as the non-RBD (COVA1-21) of the S protein (Brouwer *et al*, 2020). Therefore, we investigated whether antibodies against SARS-CoV-2 interfere with the interaction of heparan sulfates with SARS-CoV-2. We treated SARS-CoV-2 pseudovirus with different S protein targeting antibodies and measured virus binding to ACE2-negative Syndecan 1-expressing Namalwa cells. Notably, only the three neutralizing antibodies against SARS-CoV-2, COVA-1-15, 1-18, and 1-21 blocked the interaction of SARS-CoV-2 pseudovirus with Syndecan 1 in a concentration-dependent manner and to similar levels as observed for LMWH (Fig 5A). In contrast, non-neutralizing antibodies did not inhibit virus binding (Fig 5A).

Figure 3. SARS-CoV-2 infection of polarized epithelial cells is blocked by UF heparin and LMWH.

A Barrier integrity was analyzed by TEER measurements of Caco-2 and Calu-3 over a period of 20 days (n = 3 donors measured in quadruplicate).

B ACE2 cell surface expression on Caco-2 and Calu-3 was determined by quantitative real-time PCR.

C, D SARS-CoV-2 binding was measured in polarized Caco-2 (C) and Calu-3 (D) cells in presence or absence of antibodies against ACE2 (cell incubation), and UF heparin (250 IU/ml) or LMWH enoxaparin (250 IU/ml) (virus incubation).

E, F Polarized Calu-3 were inoculated with 0.5 TCID/ml of a SARS-CoV-2 isolate (hCoV-19/Italy) either directly or in presence of antibodies against ACE2 or upon pre-treatment with LMWH enoxaparin (250 IU/ml) for 30 min at 37°C. Virus was detected by lysing after 48 h through quantitative real-time PCR of viral RNA (E) and virus production was determined by detection of viral RNA in supernatant using quantitative real-time PCR (F).

Data information: Data show the mean values and error bars are the SEM. Statistical analysis was performed using (B) ordinary one-way ANOVA with Tukey's multiple-comparison test. *$P \leq 0.05$, **$P \leq 0.01$ (n = 5 Caco-2 donors measured in monoplo), *$P = 0.0460$ (n = 5 Calu-3 donors measured in monoplo), (C, D) ordinary one-way ANOVA with Tukey's multiple-comparison test. *$P \leq 0.05$, **$P \leq 0.01$, ***$P \leq 0.001$, ****$P \leq 0.0001$ (C) (n = 3 Caco-2 donors measured in triplicate), (D) (n = 3 Calu-3 donors measured in triplicate), (E, F) ordinary one-way ANOVA with Tukey's multiple-comparison test. *$P \leq 0.05$, **$P \leq 0.01$, ***$P \leq 0.001$, ****$P \leq 0.0001$ (n = 3 donors measured in monoplo). TEER: Transepithelial electrical resistance.
Source data are available online for this figure.

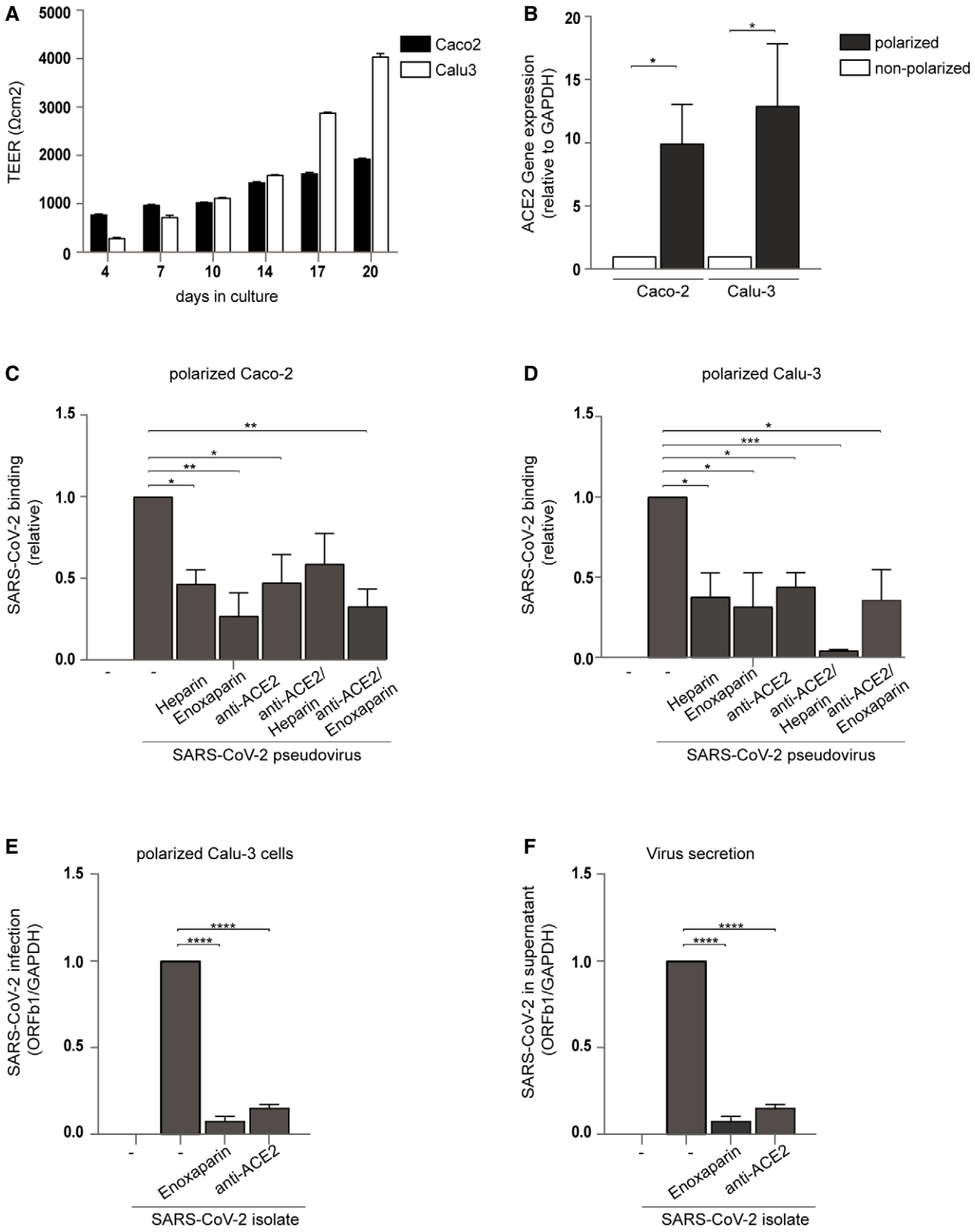

Figure 3.

Next, we determined the ability of the S protein antibodies to block binding of the primary SARS-CoV-2 isolate to ACE2-negative Syndecan 1-expressing Namalwa cells. Similar as observed for SARS-CoV-2 pseudovirus, the three neutralizing COVA antibodies blocked the interaction of the SARS-CoV-2 isolate with Syndecan 1, whereas non-neutralizing antibody COVA-1-27 did not block

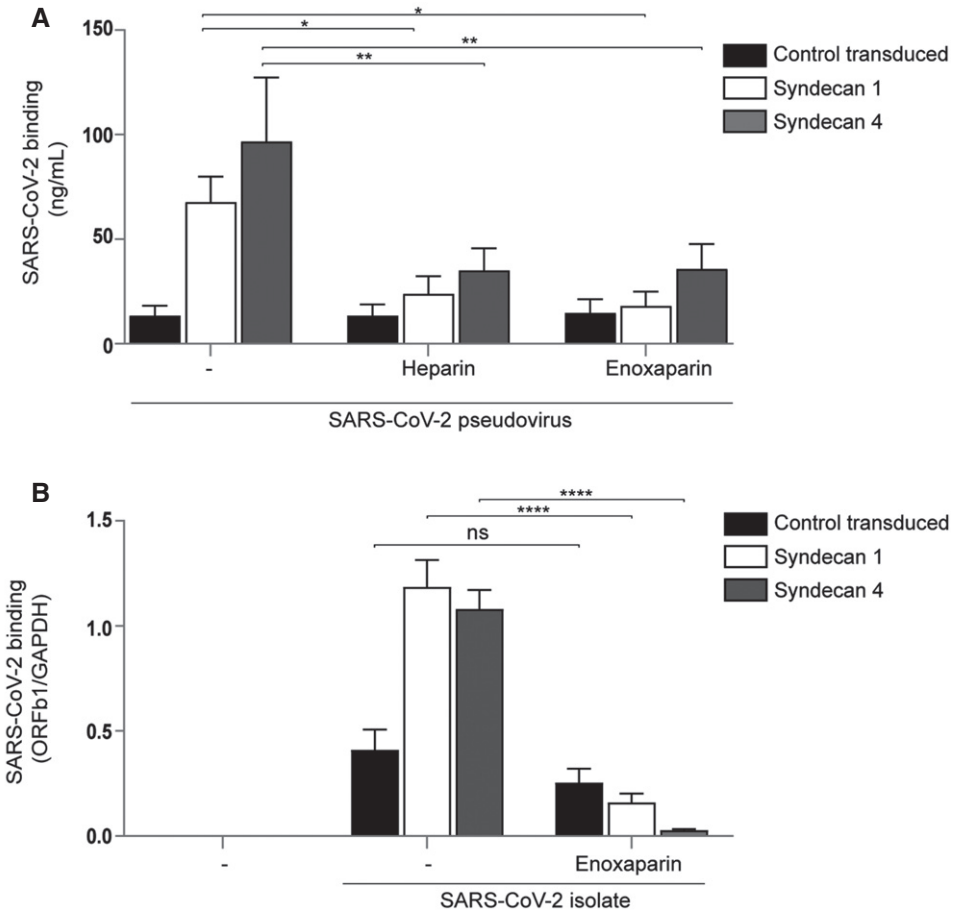

Figure 4. Heparan sulfate proteoglycans Syndecan 1 and 4 are important for SARS-CoV-2 binding.

A Namalwa cells ectopically expressing either Syndecan 1 or 4 were exposed to either SARS-CoV-2 pseudovirus alone or SARS-Cov-2 pseudovirus pre-treated with UF heparin (250 IU/ml) or LMWH enoxaparin (250 IU/ml) for 30 min at 37°C. Binding was measured after 4 h at 4°C by ELISA.

B SARS-CoV-2 isolate (hCoV-19/Italy) was pre-incubated with LMWH enoxaparin (250 IU/ml) for 30 min at 37°C. Namalwa cells expressing Syndecan 1 and 4 were exposed to either SARS-CoV-2 isolate (100 TCID/ml) or SARS-CoV-2 isolate (100 TCID/ml) pre-treated with LMWH enoxaparin (250 IU/ml) for 4 h at 4°C and binding was determined by quantitative real-time PCR.

Data information: Data show the mean values and error bars are the SEM. Statistical analysis was performed using (A) 2-way ANOVA with Dunnett's multiple-comparison test. *$P \leq 0.05$, **$P \leq 0.01$ ($n = 7$), (B) 2-way ANOVA with Sidak's multiple-comparison test. *$P \leq 0.05$, **$P \leq 0.01$, ***$P \leq 0.001$, ****$P \leq 0.0001$ ($n = 3$ measured in triplicate).

binding (Figs 5B and EV3C). These data strongly suggest that neutralizing RBD and non-RBD antibodies against SARS-CoV-2 interfere with SARS-CoV-2 binding to heparan sulfate proteoglycans and that this binding is facilitated by the SARS-CoV-2 S protein.

SARS-CoV-2 targets dendritic cells for dissemination

SARS-CoV-2 infects cells in nasal mucosa, lung, and the intestinal tract but mechanisms for dissemination of the virus from the respiratory to the intestinal tract remain unclear. Mucosal DC subsets might be involved in promoting local infection of epithelial cells in these tissues through capture as well as virus dissemination as these antigen-presenting cells after activation migrate to the lymphoid tissues to present antigens to T cells. We therefore investigated whether SARS-CoV-2 infects different mucosal DC subsets and whether DCs can transmit the virus to other cells. We differentiated monocytes to DCs, which is a model for submucosal DC, and also isolated primary human Langerhans cells (LCs) from skin (de Witte *et al*, 2007b; Sarrami-Forooshani *et al*, 2014) as this DC subset resides in squamous mucosa of different tissues including nasal and intestinal mucosa (Merad *et al*, 2008; Nijmeijer *et al*, 2019). Both monocyte-derived DCs and primary LCs efficiently bound SARS-CoV-2 pseudovirus and binding was inhibited by UF heparin as well as LMWH enoxaparin (Fig 6A and B). Notably, neither DCs nor LCs were infected by SARS-CoV-2 pseudovirus (Fig 6C), which is due to the absence of ACE2 expression on both subsets (Fig 6D). These data suggest that primary DC subsets capture SARS-CoV-2 via heparan sulfate proteoglycans but this does not lead to infection.

Different DC subsets transmit HIV-1 to target cells independent of productive infection (Geijtenbeek *et al*, 2000; Gurney *et al*,

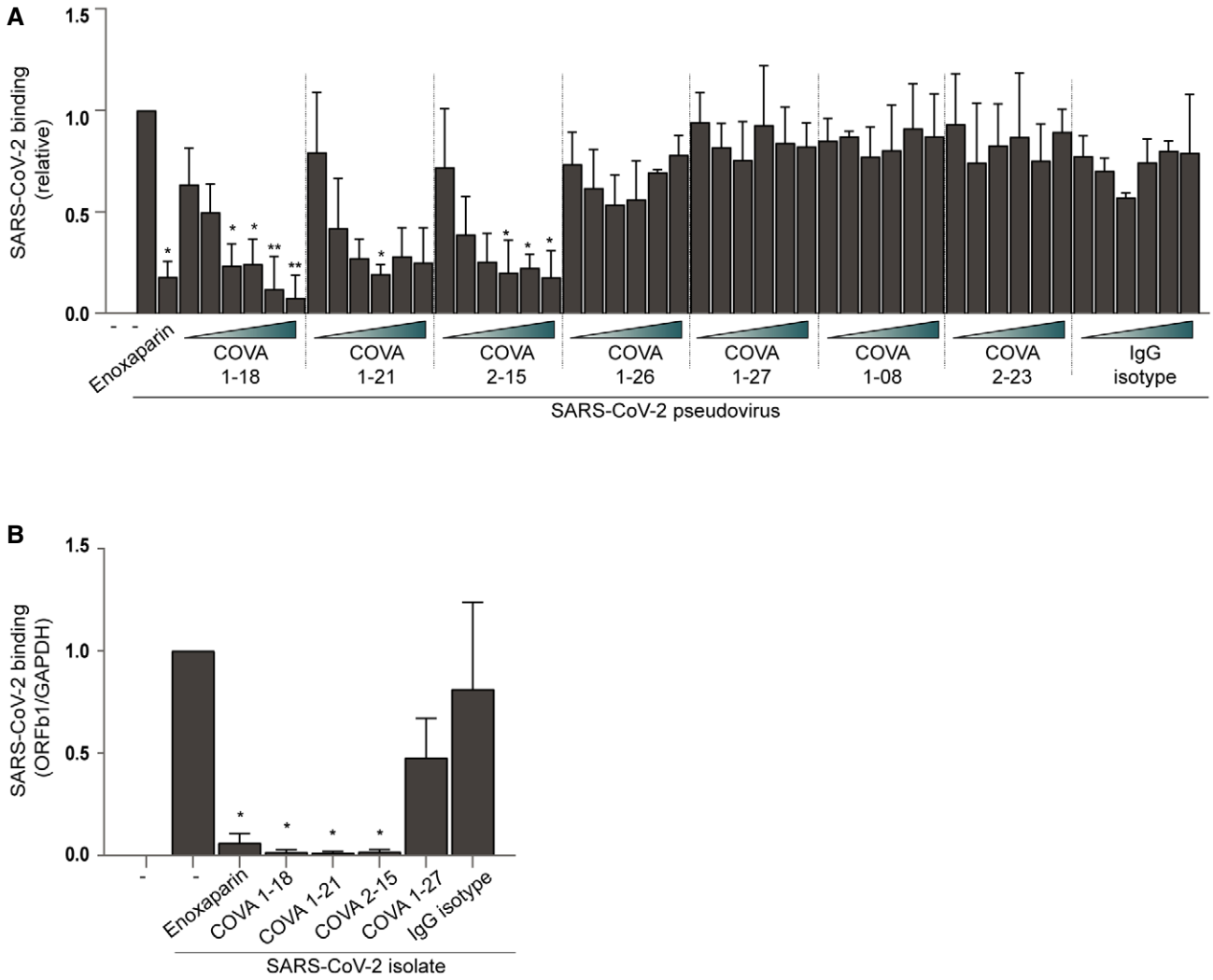

Figure 5. Neutralizing antibodies against SARS-CoV-2 interfere with SARS-CoV-2 binding to Syndecan 1.

A SARS-CoV-2 pseudovirus was pre-treated with LMWH enoxaparin (250 IU/ml), or different neutralizing antibodies against SARS-CoV-2 (COVA1-18, COVA1-21 and COVA2-15) and a human IgG1 isotype control at concentrations of 100 pg/ml, 500 pg/ml, 1 ng/ml, 5 ng/ml, 10 ng/ml, and 50 ng/ml for 30 min at 37°C. Binding of pseudovirus to Syndecan 1-expressing Namalwa cells in absence or presence of LMWH enoxaparin or antibodies was determined by ELISA.

B SARS-CoV-2 isolate (hCoV-19/Italy) was pre-treated for 30 min at 37°C with either LMWH enoxaparin (250 IU/ml) or one of the following neutralizing antibodies (COVA1-18, 1-21, and 2-15), a non-neutralizing antibody (COVA1-27), or a human IgG1 isotype control, all at the concentration of 1 pg/ml. SARS-CoV-2 isolate alone or with blocks was added at a concentration of 100 TICD/ml. Detection of virus binding to Syndecan 1-expressing Namalwa cells was measured by quantitative real-time PCR.

Data information: Data show the mean values and error bars are the SEM. Statistical analysis was performed using (A) ordinary one-way with Dunnett's multiple-comparison test. *$P \leq 0.05$, **$P \leq 0.01$ ($n = 3$), (B) ordinary one-way with Tukey's multiple-comparison test. *$P \leq 0.05$, **$P \leq 0.01$ ($n = 2$ measured in duplicate).
Source data are available online for this figure.

2005; Sarrami-Forooshani *et al*, 2014). We therefore incubated both DCs and LCs with SARS-CoV-2 pseudovirus and after washing away unbound virus, co-cultured the DC subsets with susceptible ACE2 expressing Huh7.5 cells (Fig 6E). Notably, co-culture of both virus-exposed DC subsets with Huh7.5 cells led to infection of the latter, as determined by luciferase reporter activity and infection was blocked by pre-treatment of pseudovirus with UF heparin and LMWH enoxaparin (Fig 6F and G). Next, DCs and LCs were incubated with the primary SARS-CoV-2 isolate and after extensive washing added to ACE2-positive Huh7.5 cells. Infection of Huh7.5 cells was determined by quantitative PCR after removing leftover DCs or LCs. Notably, both SARS-CoV-2-exposed DCs and LCs transmitted the virus to Huh7.5 cells as shown by infection of Huh7.5 cells, and transmission was inhibited by LMWH enoxaparin (Figs 6H and I as well as EV4A and B). These data suggest that both DCs and LCs efficiently capture SARS-CoV-2 via heparan sulfate proteoglycans and transmit the virus to ACE2 expressing target cells, which could be involved in virus dissemination from mucosal sites to lymphoid tissues.

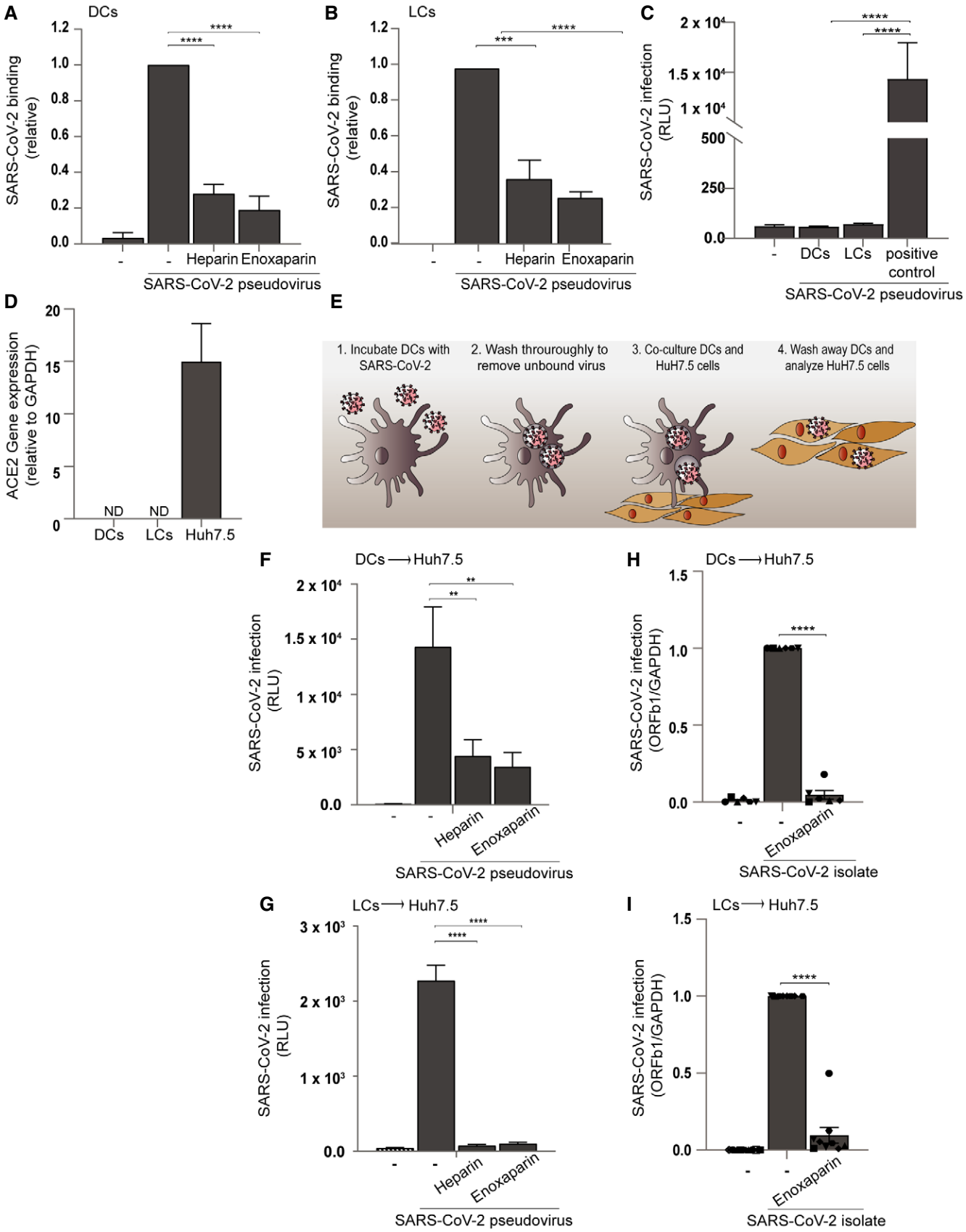
A
DCs
SARS-CoV-2 binding (relative)
Heparin
Enoxaparin
SARS-CoV-2 pseudovirus
B
LCs
C
SARS-CoV-2 infection (RLU)
DCs
LCs
positive control
D
ACE2 Gene expression (relative to GAPDH)
ND
Huh7.5
E
1. Incubate DCs with SARS-CoV-2
2. Wash throuroughly to remove unbound virus
3. Co-culture DCs and HuH7.5 cells
4. Wash away DCs and analyze HuH7.5 cells
F
DCs ⟶ Huh7.5
H
SARS-CoV-2 infection (ORFb1/GAPDH)
SARS-CoV-2 isolate
G
LCs ⟶ Huh7.5
I

Figure 6.

Figure 6. SARS-CoV-2 targets dendritic cells for dissemination.

A, B SARS-CoV-2 binding to monocyte-derived DCs (A) or primary LCs (B) in absence or presence of UF heparin (250 IU/ml) or LMWH enoxaparin (250 IU/ml).

C DCs and LCs were infected with SARS-CoV-2 pseudovirus and infection was determined after 5 days by measuring luciferase reporter activity. As positive controls, Huh7.5 cells were infected.

D ACE2 cell surface expression on DCs, LCs, and Huh7.5 cells. Representative data for an experiment repeated more than three times with similar results ($n = 3$ in duplicate).

E Graphical overview of the cell-to-cell viral transmission assay.

F, G DCs (F) and LCs (G) were pre-incubated with SARS-CoV-2 pseudovirus for 4 h at 37°C in presence or absence of UF heparin (250 IU/ml) or LMWH enoxaparin (250 IU/ml), extensively washed, and co-cultured with Huh7.5 cells. Transmission by DCs or LCs to Huh7.5 cells was determined by luciferase reporter activity.

H, I SARS-CoV-2 isolate (hCoV-19/Italy) was pre-treated with LMWH enoxaparin (250 IU/ml) for 30 min at 37°C. DCs (H) and LCs (I) were exposed to either the untreated or pre-treated SARS-CoV-2 isolate (100 TCID/ml) for 24 h, washed thoroughly, and co-cultured with Huh7.5 cells. Quantification of viral RNA was measured by quantitative real-time PCR.

Data information: Data show the mean values and error bars are the SEM. (A, B) ordinary one-way ANOVA with Tukey's multiple-comparison test. *$P \leq 0.05$, **$P \leq 0.01$, ***$P \leq 0.001$, ****$P \leq 0.0001$ (A) ($n = 4$), (B) ($n = 4$), (C) ordinary one-way ANOVA with Tukey's multiple-comparison test. *$P \leq 0.05$, **$P \leq 0.01$, ***$P \leq 0.001$, ****$P \leq 0.0001$ ($n = 4$ measured in triplicate), (F) ordinary one-way ANOVA with Dunnett's multiple-comparison test. *$P \leq 0.05$, **$P \leq 0.01$ ($n = 4$ measured in triplicate), (G) ordinary one-way ANOVA with Tukey's multiple-comparison test. *$P \leq 0.05$, **$P \leq 0.01$, ***$P \leq 0.001$, ****$P \leq 0.0001$ ($n = 3$ measured in triplicate). (H, I) ordinary one-way ANOVA with Tukey's multiple-comparison test. *$P \leq 0.05$, **$P \leq 0.01$, ***$P \leq 0.001$, ****$P \leq 0.0001$ (H) ($n = 3$ in duplicate), (I) ($n = 4$ in duplicate). DCs: Dendritic cells, LCs: Langerhans cells, RLU: relative light units, ND: not determined.

Source data are available online for this figure.

SARS-CoV-2 attaches to and infects primary nasal cells via heparan sulfate proteoglycans

Nasal epithelium is an important target for SARS-CoV-2 infection. Higher viral loads are detected in nasal and nasopharyngeal swabs compared with throat swabs (Wang *et al*, 2020; Tsang *et al*, 2021). Here, we isolated nasal cells from healthy volunteers by brushing the inside of the nasal cavity. Epithelial cells are a major component of the isolated cells as shown by high percentage of cells positive for the epithelial cell marker EpCAM (Fig 7A). Also, hematopoietic cells were present in the nasal cell fraction as shown by the expression of the hematopoietic cell marker CD45 (Fig 7A). Next, we analyzed Syndecan 1 and 4 transcripts in the nasal fraction as well as expression of ACE2. Especially high levels of Syndecan 1 transcripts were identified in the nasal fraction compared with those observed for polarized Calu-3 cells (Figs 7B and EV5A). ACE2 transcript were also detected, suggesting that SARS-CoV-2 could directly infect nasal cells (Figs 7B and EV5A) (Sungnak *et al*, 2020). We first investigated binding of primary SARS-CoV-2 isolate to the nasal cells. SARS-CoV-2 attached to the nasal cells from different donors and binding was blocked by LMWH enoxaparin (Figs 7C and EV5B). Primary nasal cells were exposed to SARS-CoV-2 and cultured for 24 h. Viability was not affected as measured by GAPDH expression. Notably, we observed high levels of SARS-CoV-2 ORF1b in cell lysates (Figs 7D and EV5C). Infection was inhibited by ACE2 block and, importantly, LMWH treatment blocked infection of SARS-CoV-2 as shown by decreased ORF1b in cell-lysate (Figs 7D and EV5C). These data suggest that heparan sulfate proteoglycans expressed by the nasal epithelium are involved in SARS-CoV-2 binding and infection.

Discussion

SARS-CoV-2 interacts with ACE2 to infect cells. Recent studies suggest that heparan sulfates might interact with S protein to enhance viral attachment (Clausen *et al*, 2020; Zhang *et al*, 2020). Moreover, Clausen *et al* (2020) show that heparan sulfate binding to SARS-CoV-2 facilitates ACE2 interactions. Here, we show that heparan sulfate proteoglycans on primary epithelial cells and primary dendritic cell subsets interact with both pseudotyped and primary SARS-CoV-2. We have identified Syndecan 1 and 4 as important attachment receptors for SARS-CoV-2. Interestingly, neutralizing antibodies against SARS-CoV-2 prevented the interaction of SARS-CoV-2 with Syndecan 1, suggesting that antibodies targeting the interaction of SARS-CoV-2 with heparan sulfates might also neutralize infection similarly to what was shown for antibodies against ACE2. Moreover, we identified a role for heparan sulfate proteoglycans during transmission by primary mucosal DC subsets, which is independent of infection. Both UF heparin and LWMH efficiently reduced infection and transmission of SARS-CoV-2. Moreover, we show that LMWH efficiently decrease infection of primary nasal epithelial cells. Thus, heparan sulfate proteoglycans function as attachment receptors for SARS-CoV-2 on primary epithelial and dendritic cells, and targeting these receptors might prevent infection.

Our data indicate that SARS-CoV-2 binding to polarized colorectal and respiratory epithelial cells is facilitated by heparan sulfates, supporting a role for heparan sulfate proteoglycans as attachment receptors. Moreover, infection of polarized respiratory epithelial cells by SARS-CoV-2 hCoV-19/Italy strain as well as pseudovirus was inhibited by LMWH to a similar level as anti-ACE2 antibodies. Combinations of LMWH with antibodies did not further decrease infection. These data suggest that SARS-CoV-2 attaches to cells via heparan sulfate proteoglycan, which facilitates interaction with ACE2 and subsequent infection. Indeed, treatment of SARS-CoV-2 with LMWH blocked heparan sulfate binding sites of the virus while it did not affect viral binding capacity to ACE2, suggesting that attachment of SARS-CoV-2 to heparan sulfate proteoglycans can facilitate ACE2 interaction.

Neutralizing antibodies against SARS-CoV-2 are a potential therapy for COVID-19 patients and most potent monoclonal neutralizing antibodies target the RBD site of the S protein thereby preventing interaction of S protein with ACE2 (Brouwer *et al*, 2020). However, neutralization antibodies have also been isolated that target non-RBD sites of the S protein. Indeed, COVA1-21 targets a non-RBD site as it does not seem to interfere with ACE2 (Brouwer *et al*, 2020), suggesting that it neutralizes either via another receptor or

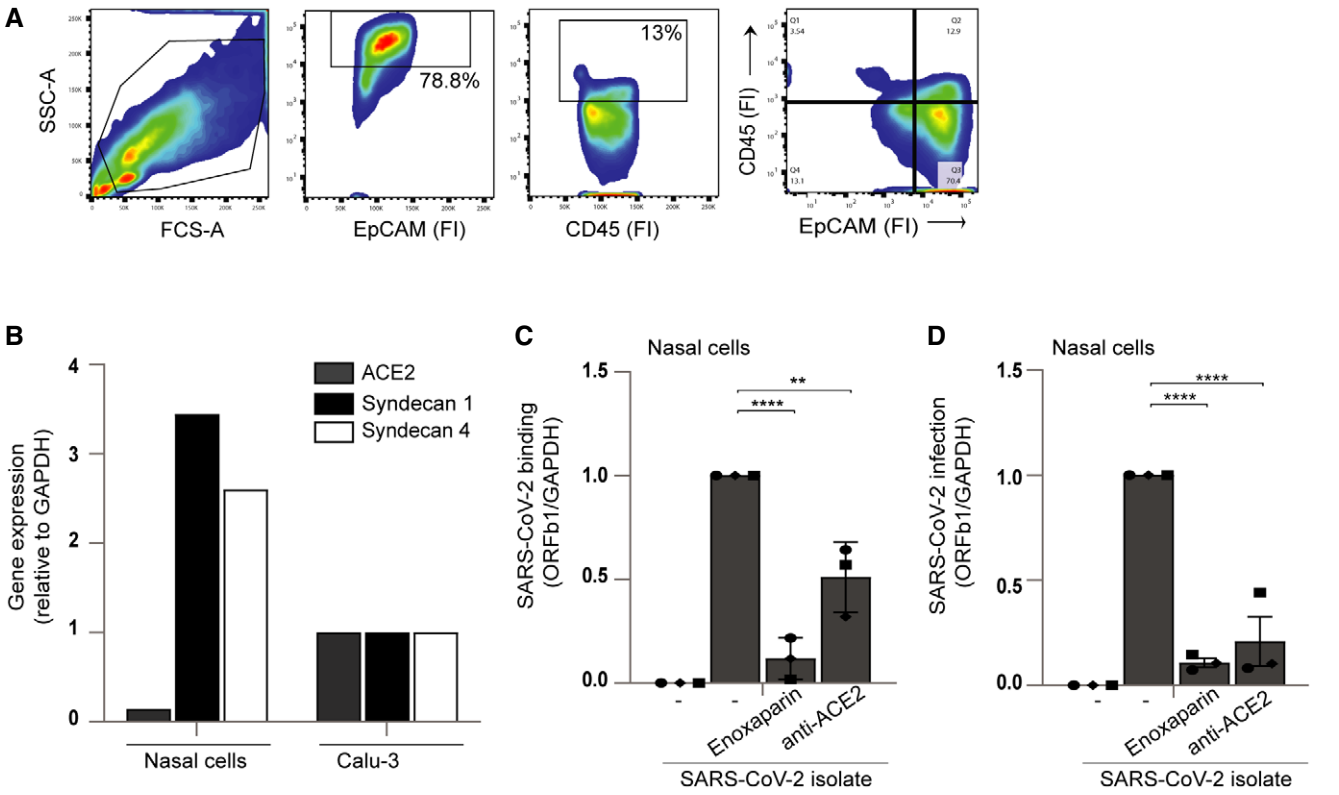

Figure 7. SARS-CoV-2 attaches to and infects primary nasal cells via heparan sulfate proteoglycans.

A Flow cytometry analysis of single-cell suspensions from the nasal epithelium. Cells were labeled with EpCAM and CD45 antibodies and gated accordingly.

B ACE2, Syndecan 1, and Syndecan 4 cell surface expression on nasal epithelial cells, compared to polarized epithelial Calu-3 cells was confirmed by quantitative real-time PCR.

C, D Nasal epithelial cells were exposed to SARS-CoV-2 isolate (hCoV-19/Italy, 100 TCID/ml) either directly or after pre-treatment with antibodies against ACE2 cell surface receptors (1 h at 37°C) or after pre-treatment with LMWH enoxaparin (250 IU/ml) for 30 min at 37°C. Detection of viral binding after 4 h at 4°C (C) and persistently infected cells lysed after 24 h at 37°C (D) was determined by quantitative real-time PCR.

Data information: Data show the mean values and error bars are the SEM. Statistical analysis was performed using (C, D) ordinary one-way ANOVA with Tukey's multiple-comparison test. *$P \leq 0.05$, **$P \leq 0.01$, ***$P \leq 0.001$, ****$P \leq 0.0001$ (C) ($n = 3$), (D) ($n = 3$ in duplicate).

another mechanism. We screened different antibodies isolated from COVID-19 patients (Brouwer *et al*, 2020) for blocking SARS-CoV-2 binding to Syndecan 1. Two RBD antibodies COVA1-18 and COVA2-15 and one non-RBD antibody COVA1-21 were identified that blocked interaction of Syndecan 1 with SARS-CoV-2 pseudovirus as well as the SARS-CoV-2 hCoV-19/Italy strain. Notably, these three antibodies are potent neutralizing antibodies against SARS-CoV-2 (Brouwer *et al*, 2020). Most non-neutralizing antibodies did not interfere with SARS-CoV-2 binding to Syndecan 1. These data suggest that blocking the interaction of SARS-CoV-2 with heparan sulfate proteoglycans might be a new mechanism of neutralization.

Our data strongly suggest that the S protein from SARS-CoV-2 is crucial to the interaction with heparan sulfate proteoglycans and Syndecan 1, as antibodies against the S protein blocked binding of both SARS-CoV-2 pseudovirus and a SARS-CoV-2 isolate to Syndecan 1-expressing Namalwa cells. Moreover, control pseudoviruses lacking the S protein did neither interact with Huh7.5 cells nor Syndecan 1-expressing cells, further supporting the specificity of the interaction between S protein from SARS-CoV-2 and heparan sulfate proteoglycans.

Different DC subsets are present in mucosal tissues to capture pathogens for antigen presentation. After pathogen interactions, DCs migrate into lymphoid tissues (Randolph *et al*, 2005). Several viruses, such as HIV-1 and Dengue virus, hijack DC functions for dissemination (Geijtenbeek *et al*, 2000; Pham *et al*, 2012). Primary LCs and DCs efficiently captured SARS-CoV-2 via heparan sulfate proteoglycans. Previously we have shown that LCs express Syndecan 4 (Nijmeijer *et al*, 2020) and DCs express Syndecan 3 and Syndecan 4 (de Witte *et al*, 2007a). Thus, our data suggest that both Syndecan 3 and 4 might be involved in SARS-CoV-2 capture. Both LCs and DCs did not express ACE2 and were not infected by SARS-CoV-2 pseudovirus. However, co-culture of SARS-CoV-2-exposed LCs and DCs with ACE2 cells led to productive infection with pseudotyped as well as a primary SARS-CoV-2 strain. Transmission was blocked by LMWH suggesting that capture by heparan sulfate proteoglycans is important for transmission. Moreover, our data indicate that SARS-CoV-2 transmission is independent of direct infection of DC subsets, suggesting that this might allow the virus from escaping neutralization by antibodies or antiviral drugs. However, the exact mechanism of this viral transfer are still not entirely clear.

The upper airways and nasal epithelium might be the primary route of infection as higher viral load have been found in nasal swabs when compared to throat swabs (Zou *et al*, 2020a). Moreover, nasal epithelial cells express ACE2 and the cellular serine protease TMPRSS2 (Sungnak *et al*, 2020). We have isolated nasal cells from healthy volunteers using a nasal brush and the majority of cells were EpCAM-positive epithelial cells and some hematopoietic cells, most likely lymphocytes and myeloid cells. Syndecan 1 and 4 transcripts were detected at high levels in nasal cell fraction, suggesting that Syndecans might be involved in virus interactions. Our data support an important role for nasal cells as the first target for SARS-CoV-2 as nasal cells efficiently captured primary SARS-CoV-2 and were also infected by SARS-CoV-2. LMWH blocked capture and infection of the nasal cells. Interestingly, the nasal cells were not cultured as done in previous studies (Müller *et al*, 2013; Vanders *et al*, 2019) suggesting that the nasal epithelial cells are a direct target for SARS-CoV-2 and that heparan sulfate proteoglycans are involved in the infection.

LMWH are already used as subcutaneous treatment of COVID-19 patients to prevent systemic clotting (World Health Organization, 2020a; Zhai *et al*, 2020). Interestingly, here we have identified an important ability of LMWH to directly block SARS-CoV-2 binding and infection of epithelial cells as well as preventing virus transmission. Our data support the use of LMWH as prophylactic treatment for SARS-CoV-2 as well as a treatment option early in infection to block further infection and dissemination. Vaccination programs are currently running worldwide but it remains unclear whether this is sufficient for specific patients who are immunocompromised or suffer from other diseases that prevent an efficient immune response upon vaccination. LMWH prophylaxis might also be used when new SARS-CoV-2 variants arise that are not efficiently counteracted by the current vaccines.

Materials and Methods

Reagents and antibodies

The following antibodies were used (all anti-human): ACE2 (R&D), (Heparan Sulfate (clone F58-10E4) (Amsbio), digested Heparan (clone F69-3G10) (Amsbio), CD1a-APC mouse IgG1 (BD Biosciences, San Jose, CA, USA), CD207-PE (langerin) mouse IgG1 (#IM3577), PerCP-Cy™5.5-conjugated mouse IgG1 EPCAM 347199) (BD Bioscience), PE-conjugated mouse IgG1 E-Cadherin (FAB18381P) (R&D Systems), APCcy-conjugated mouse IgG1 CD45 (557833) (BD Bioscience), APC-conjugated CD14 (21620146sp) (Immunotools), PE-conjugated mouse IgG1 CD11b (101208) (Biolegend). FITC-conjugated goat-anti-mouse IgM (#31992) (Invitrogen), AF488-conjugated donkey-anti-mouse IgG2b (Invitrogen). Flow cytometric analyses were performed on a BD FACS Canto II (BD Biosciences). Data were analyzed using FlowJo vX.0.7 software (TreeStar).

The following reagents were used: unfractionated (UF) heparin, 5.000 IE/ml (LEO). low molecular weight heparins (LMWH): dalteparin, 10.000 IE anti-Xa/ml (Pfizer), tinzaparin, 10.000 IE anti-X1/0.5 ml (LEO), enoxaparin, 6000 IE (60 mg)/0.6 ml (Sanofi), nadroparin, 9.500 IE anti-XA/ml (Aspen). Heparinase III from *Flavobacterium heparium*, EC 4.2.2.8, Batch 010, (Amsbio). Biotinylated SARS-CoV-2 S protein as well as neutralizing and non-neutralizing COVA antibodies was generated as described previously (Brouwer *et al*, 2020).

Cell lines

The Simian kidney cell line VeroE6 (ATCC® CRL-1586™) was maintained in CO_2 independent medium (Gibco Life Technologies, Gaithersburg, Md.) supplemented with 10% fetal calf serum (FCS), L-glutamine, and penicillin/streptomycin (10 μg/mL). Culture was maintained at 37C without CO_2. Huh7.5 (human hepatocellular carcinoma) cells received from Dr. Charles M. Rice (Lindenbach *et al*, 2005) were maintained in Dulbecco's modified Eagle's medium (Gibco Life Technologies) containing 10% fetal calf serum (FCS), L-glutamine, and penicillin/streptomycin (10 μg/ml). Medium was supplemented with 1mM Hepes buffer (Gibco Life Technologies). The human B cell line Namalwa (ATCC, CRL-1432) and Namalwa cells stably expressing human Syndecan 1, Syndecan 2, Syndecan 3 and Syndecan 4 (Zhang *et al*, 2001) were a gift from Dr. Guido David and Dr. Philippe A Gallay. The cells were maintained in RPMI 1640 medium (Gibco Life Technologies) containing 10% fetal calf serum (FCS), penicillin/streptomycin (10 μg/ml), and 1 mM sodium pyruvate (Thermo Fisher). The expression of the different Syndecans was validated by PCR analysis using specific primers aimed against Syndecans. The human multiple myeloma cell line XG-1 was cultured in Iscove's modified Dulbecco's medium (Invitrogen Life Technologies) containing 10% fetal bovine serum, 100 U/ml of penicillin, and 100 μg/ml of streptomycin. The medium was further was supplemented with 500 pg/ml of interleukin 6 (Prospec). The CRISPR-Cas9 knockout for *Ext1* has been described previously (Ren *et al*, 2018). The human embryonic kidney 293T/17 cells (ATCC, CRL-11268) were maintained in Dulbecco's modified Eagle's medium (Gibco Life Technologies) containing 10% fetal calf serum (FCS), L-glutamine, and penicillin/streptomycin (10 μg/ml). The human epithelial Caco-2 cells (ATCC, HTB-37™) as well as the human lung epithelial Calu-3 cells (ATCC® HTB-55™) were maintained in Dulbecco's modified Eagle's medium (Gibco Life Technologies) containing 10% fetal calf serum (FCS), L-glutamine, and penicillin/streptomycin (10 μg/ml) and supplemented with MEM non-essential amino acids solution (NEAA) (Gibco Life Technologies). To create a monolayer of polarized cells, Caco-2 and Calu-3 cells were maintained in 6.5 mm Transwell® with 5.0 μm pore polycarbonate membrane insert (Corning). The cells were initially seeded with a density of 25.000 cells per 6.5 mm filter insert and full polarization was reached after 2 weeks in culture. Polarization was monitored by measuring transepithelial electrical resistance (TEER).

Primary human cells

This study has been conducted in accordance with the ethical principles set out in the Declaration of Helsinki and was approved by the institutional review board of the Academic Medical Center (AMC, Amsterdam, Netherlands) and the Ethics Advisory Body of the Sanquin Blood Supply Foundation (Amsterdam, Netherlands).

$CD14^+$ monocytes were isolated from the blood of healthy volunteer donors (Sanquin blood bank) and subsequently differentiated into monocyte-derived DCs as described previously (Mesman *et al*, 2014) (Fig EV2E). LCs were isolated from human epidermal sheets obtained from healthy donors after plastic surgery. Epidermal sheets

were prepared as described previously (de Witte *et al*, 2007b; Sarrami-Forooshani *et al*, 2014). Briefly, skin grafts were obtained using a dermatome (Zimmer Biomet, Indiana USA). After incubation with Dispase II (1 U/ml, Roche Diagnostics), epidermal sheets were separated from dermis, washed, and cultured in IMDM (Thermo Fischer Scientific, USA) supplemented with 10% FCS, gentamicin (20 μg/ml, Centrafarm, Netherlands), penicillin/streptomycin (10 U/ml and 10 μg/ml, respectively; Invitrogen) for 3 days after which LCs were harvested. Purity of LCs was routinely verified by flow cytometry using antibodies directed against CD207 (langerin) and CD1a (Fig EV2F).

Primary nasal epithelial cells were obtained from healthy volunteers. Cells were isolated from the lower nasal cavity with a brush after which they were transferred into CO_2 independent medium (Gibco Life Technologies) supplemented with 10% fetal calf serum (FCS), L-glutamine, and penicillin/streptomycin (10 μg/ml). Cell surface receptor expression was determined by flow cytometry.

SARS-Cov-2 pseudovirus production

For production of single-round infection viruses, human embryonic kidney 293T/17 cells (ATCC, CRL-11268) were co-transfected with an adjusted HIV-1 backbone plasmid (pNL4-3.Luc.R-S-) containing previously described stabilizing mutations in the capsid protein (PMID: 12547912) and a firefly luciferase gene in the *nef* open reading frame (1.35 μg) and pSARS-CoV-2 expressing SARS-CoV-2 S protein (0.6 μg) (GenBank; MN908947.3) (Brouwer *et al*, 2020). For single-round infection viruses lacking S protein, an empty vector (pcDNA3.1(+), Thermo Fisher Scientific, #V79020.) was added instead. Transfection was performed in 293T/17 cells using GeneJuice (Novagen, USA) transfection kit according to the manufacturer's protocol. At day 3 or day 4, pseudotyped SARS-CoV-2 virus particles were harvested and filtered over a 0.2-μm nitrocellulose membrane (Sartorius Stedim, Gottingen, Germany). SARS-CoV-2 pseudovirus productions were quantified by p24 ELISA (Perkin Elmer Life Sciences).

SARS-CoV-2 production

All experiments with SARS-CoV-2 isolates were performed in a BSL-3 laboratory, following all appropriate safety and security protocols approved by the Amsterdam UMC BioSafetyGroep and performed under the environmental license obtained from the municipality Amsterdam. The following reagent was obtained from Dr. Maria R. Capobianchi through BEI Resources, NIAID, NIH: SARS-Related Coronavirus 2, Isolate Italy-INMI1, NR-52284, originally isolated January 2020 in Rome, Italy. VeroE6 cells (ATCC® CRL-1586™) were inoculated with the SARS-CoV-2 isolate and used for reproduction of virus stocks. Cytopathic effect (CPE) formation was closely monitored and virus supernatant was harvested after 48 h. Viral titers were determined by tissue culture infectious dose (TCID50) on VeroE6 cells. In brief, VeroE6 cells were seeded in a 96-well plate at a cell density of 8,000 cells in 100 μl. After 24 h, cells were inoculated with a fivefold serial dilution of SARS-CoV-2 isolate in quadruplicate. Cell cytotoxicity was measured using the MTT assay 48 h after infection. Loss of MTT staining as determined by spectrometer (OD 580 nm) is indicative of the (CPE) of SARS-CoV-2. The virus titer was determined as TCID50/ml and calculated based on the Reed Muench method (Reed & Muench, 1938).

Pseudovirus infection assays

HuH7.5 and 293T cells were exposed to 95 ng of single-round SARS-CoV-2 pseudovirus. Primary dendritic cell subsets were exposed to 190 ng and polarized Caco2 and Calu3 cells to 477.62 ng of single-round SARS-CoV-2 pseudovirus. Virus was pre-incubated with 250 IU/ml LMWH or UF heparin to addition to the cells. Viral protein production was quantified after 5 days at 37°C by measuring luciferase reporter activity. Luciferase activity (relative light units (R.L.U.)) was measured using the Luciferase assay system (Promega, USA) according to the manufacturer's instructions.

Virus binding

In order to determine SARS-CoV-2 binding, target cells were seeded in a 96-well plate at a density of either 10,000 cells in 100 μl for adherent cells the day before or 100,000 cells in 100 μl for suspension cells the same day. All cells were exposed to either 95 ng/ml of SARS-CoV-2 pseudovirus or SARS-CoV-2 isolate (hCoV-19/Italy, 100 TCID/ml) for 4 h at 4°C. After 4 h, cells were washed extensively to remove unbound virus. Cells incubated with SARS-Cov-2 pseudovirus were lysed and binding and internalization were quantified by RETRO-TEK HIV-1 p24 ELISA according to manufacturer instructions (ZeptoMetrix Corporation). Cells incubated with SARS-Cov-2 isolate (hCoV-19/Italy) were lysed with AVL buffer and RNA was isolated with the QIAamp Viral RNA Mini Kit (Qiagen) according to the manufacturer's protocol.

SARS-CoV-2 WT infection

VeroE6 cells were seeded at a density of 10,000 cells in 100 μl in a 96-well plate. After 24 h, the cells were exposed to the SARS-CoV-2 isolate (hCoV-19/Italy, 100 TCID/ml) for 48 h. Additionally, SARS-CoV-2 isolate was pre-incubated with 250 IU/ml of LMWH enoxaparin prior to cell inoculation. Infection was measured after 48 h at 37°C by MTT and determined by cell viability. Polarized Calu-3 cells that had initially been seeded with 250,000 cells/transwell (6.5 mm filter insert) prior to infection were incubated with SARS-CoV-2 isolate (hCoV-19/Italy, 0.5 TCID/ml) for 24 h, after which cells were washed thoroughly and new medium was added. Viral infection and secretion were determined by RT-PCR measurement of ORF-1b transcript. Primary nasal epithelial cells seeded at a density of 50,000–100,000 cells in 100 μl were incubated with SARS-CoV-2 isolate (hCoV-19/Italy, 100 TCID/ml) for 24 h after which ORF-1b transcript was determined by RT-PCR.

Tetrazolium dye colorimetric cell viability (MTT) assay

MTT solution was added to VeroE6 cells and incubated for 2 h at 37°C. After removing the MTT solution, MTT solvent containing 4 mM HCl and 1% Nonidet P-40 (NP40) in isopropanol was added to the cells. Homogenous solution was measured at optical density between 580 and 655 nm.

293T Transfection with ACE2

To generate cells expressing human ACE2, human embryonic kidney 293T/17 cells were transfected with pcDNA3.1(−)hACE2

(Addgene plasmid #1786). Transfection was performed in 293T/17 cells using the GeneJuice (Novagen, USA) transfection kit according to the manufacturer's protocol. At 24 h post-transfection, cells were washed with phosphate-buffered saline (PBS) and cultured for recovering at 37°C for 24 h in Dulbecco's MEM supplemented with 10% heat-inactivated fetal calf serum (FCS), L-glutamine, and penicillin/streptomycin (10 U/ml) After 24 h of recovery, cells were cultured in media supplemented with G418 (5 mg/ml) (Thermo Fisher) and passage for 3 weeks at 37°C. Surviving clones were analyzed for ACE2 expression via flow cytometry and quantitative real-time PCR.

Transmission assays and co-culture

Per condition, 100,000 DCs or LCs/100 µl were exposed to 191.05 ng of pseudotyped SARS-CoV-2 or pseudotyped SARS-CoV-2 pre-incubated with 250 IU/ml UF heparin or LMWH enoxaparin for 30 min at 37°C. After 4 h at 37°C, cells were harvested, extensively washed to remove unbound virus, and co-cultured with Huh7.5 for 5 days at 37°C. After 5 days, DCs or LCs were washed away and Huh7.5 cells were analyzed with the Luciferase assay system (Promega, USA) according to the manufacturer's instructions to determine infection based on luciferase reporter activity. Similarly, DCs or LCs were also exposed to either SARS-CoV-2 isolate (hCoV-19/Italy, 100 TCID/ml) or SARS-Cov-2 isolate pre-incubated with 250 IU/ml LMWH enoxaparin (30 min at 37°C). After 24 h at 37°C, cells were extensively washed to remove unbound virus and co-cultured with HuH7.5 for 24 h at 37°C. Subsequently, Huh7.5 cells were again washed extensively to remove DCs or LCs and Huh7.5 cells were lysed for isolation of viral RNA.

RNA isolation and quantitative real-time PCR

Viral RNA in cells and supernatant was isolated with the QIAamp Viral RNA Mini Kit (Qiagen) according to the manufacturer's protocol. cDNA was synthesized with the M-MLV reverse transcriptase kit (Promega) and diluted 1 in 5 before further application. Cellular mRNA of cells not exposed to virus was isolated with an mRNA Capture kit (Roche) and cDNA was synthesized with a reverse transcriptase kit (Promega). PCR amplification was performed in the presence of SYBR green in a 7500 Fast Realtime PCR System (ABI). Specific primers were designed with Primer Express 2.0 (Applied Biosystems). Primer sequences used for mRNA expression were for gene product: GAPDH, forward primer (CCATGTTCGT CATGGGTGTG), reverse primer (GGTGCTAA GCAGTTGGTGGTG). For gene product SARS-CoV-2 ORf1b, forward primer (TGGGGTTTTACAGGTAACCT), reverse primer (AACACGCTTAAC AAAGCACTC) as described previously (Chu *et al*, 2020). For gene product: ACE2, forward primer (GGACCCAGGAAATGTTCAGA), reverse primer (GGCTGCAGAAAGTGACATGA). For gene product: Syndecan 1, forward primer (ATCACCTTGTCACAGCAGACCC) reverse primer (CTCCACTTCTGGCAGGACTACA). Syndecan 4, forward primer (AGGTGTCAATGTCCAGCACTGTG) reverse primer (AGCAGTAGGATCAGGAAGACGGC). The normalized amount of target mRNA was calculated from the Ct values obtained for both target and household mRNA with the equation Nt = 2Ct (GAPDH) − Ct(target). For relative mRNA expression, control siRNA sample was set at 1 for each donor.

Biosynthesis inhibition and enzymatic treatment

HuH7.5 cells were treated in D-PBS/0.25% BSA with 46 milliunits heparinase III (Amsbio) for 1 h at 37°C, washed, and used in subsequent experiments. Enzymatic digestion was verified by flow cytometry using antibodies directed against heparan sulfates and digested heparan sulfates.

Human ACE2 protein binding

Recombinant human ACE2 protein, kindly provided by the laboratory of Dr. Rogier Sanders, was coated at a concentration of 2 µg/ml on a high binding plate (Nunc MaxiSorp™ flat-bottom, Thermo Fisher) at 4°C. After overnight incubation, wells were blocked with 2% BSA for 30 min at 37°C before being washed extensively. SARS-Cov-2 isolate (hCoV-19/Italy, 20,000 TCID/ml) was added for 4 h at 4°C at a total of 50 µl. After 4 h, wells were lysed and SARS-CoV-2 ORF-1b transcript was determined by quantitative real-time PCR.

Statistics

All results are presented as mean ± SEM and were analyzed by GraphPad Prism 8 software (GraphPad Software Inc.). A two-tailed, parametric Student's *t*-test for paired observations (differences within the same donor) or unpaired observation, Mann–Whitney tests (differences between different donors that were not normally distributed) was performed. For unpaired, non-parametric observations, a one-way ANOVA or two-way ANOVA test with post hoc analysis (Tukey's or Dunnet's) was performed. Statistical significance was set at $*P < 0.05$, $**P < 0.01$, $***P < 0.001$, $****P < 0.0001$.

Data availability

This study includes no data deposited in external repositories.

Expanded View for this article is available online.

Acknowledgements
We thank Jonne Snitselaar and Yoann Aldon for help with production of antibodies and Hildo Lantermans for help with the XG1/EXT1 KO cell lines. This research was funded by the Netherlands Organisation for Health Research and Development (ZonMw) together with the Stichting Proefdiervrij (ZonMw MKMD COVID-19 grant nr. 114025008 to TBHG), ZonMw (446002508 to GJB) and European Research Council (Advanced grant 670424 to TBHG), Amsterdam UMC PhD grant and two COVID-19 grants from the Amsterdam institute for Infection & Immunity (to TBHG, RWS, and MJG). This study was also supported by the Netherlands Organization for Scientific Research (NWO) through a Vici grant (to RWS), and by the Bill & Melinda Gates Foundation through the Collaboration for AIDS Vaccine Discovery (CAVD), grant INV-002022 (to RWS).

Author contributions
MB-J and JE conceived and designed experiments. MB-J, JE, TMK, LCH, JLH performed the experiments and contributed to scientific discussion. PJMB, KEV, MS, GJB, BMN, NAK, MJG, and RWS contributed essential research materials and scientific input. MB-J, JE, TMK, and TBHG analyzed and interpreted data.

JE, MB-J, and TBHG wrote the manuscript with input from all listed authors. TBHG was involved in all aspects of the study.

Conflict of interest

The authors declare that they have no conflict of interest.

References

Agha M, Blake M, Chilleo C, Wells A, Haidar G (2021) Suboptimal response to COVID-19 mRNA vaccines in hematologic malignancies patients. *medRxiv* https://doi.org/10.1101/2021.04.06.21254949 [PREPRINT]

Artursson P, Palm K, Luthman K (2001) Caco-2 monolayers in experimental and theoretical predictions of drug transport. *Adv Drug Deliv Rev* 46: 27 – 43

Bacsa S, Karasneh G, Dosa S, Liu J, Valyi-Nagy T, Shukla D (2011) Syndecan-1 and syndecan-2 play key roles in herpes simplex virus type-1 infection. *J Gen Virol* 92: 733 – 743

Bosch BJ, van der Zee R, de Haan CA, Rottier PJ (2003) The coronavirus spike protein is a class I virus fusion protein: structural and functional characterization of the fusion core complex. *J Virol* 77: 8801 – 8811

Boyarsky BJ, Ruddy JA, Connolly CM, Ou MT, Werbel WA, Garonzik-Wang JM, Segev DL, Paik JJ (2021) Antibody response to a single dose of SARS-CoV-2 mRNA vaccine in patients with rheumatic and musculoskeletal diseases. *Ann Rheum Dis* 80: 1098 – 1099

Brooks SK, Webster RK, Smith LE, Woodland L, Wessely S, Greenberg N, Rubin GJ (2020) The psychological impact of quarantine and how to reduce it: rapid review of the evidence. *Lancet* 395: 912 – 920

Brouwer PJM, Caniels TG, van der Straten K, Snitselaar JL, Aldon Y, Bangaru S, Torres JL, Okba NMA, Claireaux M, Kerster G *et al* (2020) Potent neutralizing antibodies from COVID-19 patients define multiple targets of vulnerability. *Science* 369: 643 – 650

Burkard C, Verheije MH, Wicht O, van Kasteren SI, van Kuppeveld FJ, Haagmans BL, Pelkmans L, Rottier PJ, Bosch BJ, de Haan CA (2014) Coronavirus cell entry occurs through the endo-/lysosomal pathway in a proteolysis-dependent manner. *PLoS Pathog* 10: e1004502

Byrnes AP, Griffin DE (1998) Binding of Sindbis virus to cell surface heparan sulfate. *J Virol* 72: 7349 – 7356

Chu DKW, Pan Y, Cheng SMS, Hui KPY, Krishnan P, Liu Y, Ng DYM, Wan CKC, Yang P, Wang Q *et al* (2020) Molecular diagnosis of a novel coronavirus (2019-nCoV) causing an outbreak of pneumonia. *Clin Chem* 66: 549 – 555

Clausen TM, Sandoval DR, Spliid CB, Pihl J, Perrett HR, Painter CD, Narayanan A, Majowicz SA, Kwong EM, McVicar RN *et al* (2020) SARS-CoV-2 infection depends on cellular heparan sulfate and ACE2. *Cell* 183: 1043 – 1057

Collier DA, De Marco A, Ferreira IATM, Meng BO, Datir RP, Walls AC, Kemp SA, Bassi J, Pinto D, Silacci-Fregni C *et al* (2021) Sensitivity of SARS-CoV-2 B.1.1.7 to mRNA vaccine-elicited antibodies. *Nature* 593: 136 – 141

Ferioli M, Cisternino C, Leo V, Pisani L, Palange P, Nava S (2020) Protecting healthcare workers from SARS-CoV-2 infection: practical indications. *Eur Respir Rev* 29: 200068

Geijtenbeek TBH, Kwon DS, Torensma R, van Vliet SJ, van Duijnhoven GCF, Middel J, Cornelissen ILMHA, Nottet HSLM, KewalRamani VN, Littman DR *et al* (2000) DC-SIGN, a dendritic cell-specific HIV-1-binding protein that enhances trans-infection of T cells. *Cell* 100: 587 – 597

Gurney KB, Elliott J, Nassanian H, Song C, Soilleux E, McGowan I, Anton PA, Lee B (2005) Binding and transfer of human immunodeficiency virus by DC-SIGN+ cells in human rectal mucosa. *J Virol* 79: 5762 – 5773

Hamming I, Timens W, Bulthuis ML, Lely AT, Navis G, van Goor H (2004) Tissue distribution of ACE2 protein, the functional receptor for SARS coronavirus. A first step in understanding SARS pathogenesis. *J Pathol* 203: 631 – 637

Harapan H, Itoh N, Yufika A, Winardi W, Keam S, Te H, Megawati D, Hayati Z, Wagner AL, Mudatsir M (2020) Coronavirus disease 2019 (COVID-19): a literature review. *J Infect Public Health* 13: 667 – 673

Harcourt JL, Caidi H, Anderson LJ, Haynes LM (2011) Evaluation of the Calu-3 cell line as a model of in vitro respiratory syncytial virus infection. *J Virol Methods* 174: 144 – 149

Hayashida K, Johnston DR, Goldberger O, Park PW (2006) Syndecan-1 expression in epithelial cells is induced by transforming growth factor beta through a PKA-dependent pathway. *J Biol Chem* 281: 24365 – 24374

Hoffmann M, Kleine-Weber H, Schroeder S, Krüger N, Herrler T, Erichsen S, Schiergens TS, Herrler G, Wu N-H, Nitsche A *et al* (2020) SARS-CoV-2 cell entry depends on ACE2 and TMPRSS2 and is blocked by a clinically proven protease inhibitor. *Cell* 181: 271 – 280

Hui KPY, Cheung M-C, Perera RAPM, Ng K-C, Bui CHT, Ho JCW, Ng MMT, Kuok DIT, Shih KC, Tsao S-W *et al* (2020) Tropism, replication competence, and innate immune responses of the coronavirus SARS-CoV-2 in human respiratory tract and conjunctiva: an analysis in ex-vivo and in-vitro cultures. *Lancet Respir Med* 8: 687 – 695

Hulswit RJ, de Haan CA, Bosch BJ (2016) Coronavirus spike protein and tropism changes. *Adv Virus Res* 96: 29 – 57

Jiang J, Cun W, Wu X, Shi Q, Tang H, Luo G (2012) Hepatitis C virus attachment mediated by apolipoprotein E binding to cell surface heparan sulfate. *J Virol* 86: 7256 – 7267

Kakkar AK (2004) Low- and ultra-low-molecular-weight heparins. *Best Pract Res Clin Haematol* 17: 77 – 87

Lamers MM, Beumer J, van der Vaart J, Knoops K, Puschhof J, Breugem TI, Ravelli RBG, Paul van Schayck J, Mykytyn AZ, Duimel HQ *et al* (2020) SARS-CoV-2 productively infects human gut enterocytes. *Science* 369: 50 – 54

Letko M, Marzi A, Munster V (2020) Functional assessment of cell entry and receptor usage for SARS-CoV-2 and other lineage B betacoronaviruses. *Nat Microbiol* 5: 562 – 569

Li F, Li W, Farzan M, Harrison SC (2005) Structure of SARS coronavirus spike receptor-binding domain complexed with receptor. *Science* 309: 1864 – 1868

Lindenbach BD, Evans MJ, Syder AJ, Wölk B, Tellinghuisen TL, Liu CC, Maruyama T, Hynes RO, Burton DR, McKeating JA *et al* (2005) Complete replication of hepatitis C virus in cell culture. *Science* 309: 623 – 626

Mathieu E, Ritchie H, Ortiz-Ospina E, Roser M, Hasell J, Appel C, Giattino C, Rodés-Guirao L (2021) A global database of COVID-19 vaccinations. *Nat Hum Behav* 5: 947 – 953

Merad M, Ginhoux F, Collin M (2008) Origin, homeostasis and function of Langerhans cells and other langerin-expressing dendritic cells. *Nat Rev Immunol* 8: 935 – 947

Mesman AW, Zijlstra-Willems EM, Kaptein TM, de Swart RL, Davis ME, Ludlow M, Duprex WP, Gack MU, Gringhuis SI, Geijtenbeek TB (2014) Measles virus suppresses RIG-I-like receptor activation in dendritic cells via DC-SIGN-mediated inhibition of PP1 phosphatases. *Cell Host Microbe* 16: 31 – 42

Milewska A, Zarebski M, Nowak P, Stozek K, Potempa J, Pyrc K (2014) Human coronavirus NL63 utilizes heparan sulfate proteoglycans for attachment to target cells. *J Virol* 88: 13221 – 13230

Müller L, Brighton LE, Carson JL, Fischer 2nd WA, Jaspers I (2013) Culturing of human nasal epithelial cells at the air liquid interface. *J Vis Exp* e50646

Nicola M, Alsafi Z, Sohrabi C, Kerwan A, Al-Jabir A, Iosifidis C, Agha M, Agha R (2020) The socio-economic implications of the coronavirus pandemic (COVID-19): a review. *Int J Surg* 78: 185 – 193

Nijmeijer BM, Eder J, Langedijk CJM, Kaptein TM, Meeussen S, Zimmermann P, Ribeiro CMS, Geijtenbeek TBH (2020) Syndecan 4 upregulation on activated langerhans cells counteracts langerin restriction to facilitate hepatitis C virus transmission. *Front Immunol* 11: 503

Nijmeijer BM, Sarrami-Forooshani R, Steba GS, Schreurs RR, Koekkoek SM, Molenkamp R, Schinkel J, Reiss P, Siegenbeek van Heukelom ML, van der Valk M *et al* (2019) HIV-1 exposure and immune activation enhance sexual transmission of Hepatitis C virus by primary Langerhans cells. *J Int AIDS Soc* 22: e25268

Peiris JS, Yuen KY, Osterhaus AD, Stöhr K (2003) The severe acute respiratory syndrome. *N Engl J Med* 349: 2431 – 2441

Pham AM, Langlois RA, TenOever BR (2012) Replication in cells of hematopoietic origin is necessary for Dengue virus dissemination. *PLoS Pathog* 8: e1002465

Randolph GJ, Angeli V, Swartz MA (2005) Dendritic-cell trafficking to lymph nodes through lymphatic vessels. *Nat Rev Immunol* 5: 617 – 628

Reed LJ, Muench H (1938) A simple method of estimating fifty per cent endpoints. *Am J Epidemiol* 27: 493 – 497

Ren Z, van Andel H, de Lau W, Hartholt RB, Maurice MM, Clevers H, Kersten MJ, Spaargaren M, Pals ST (2018) Syndecan-1 promotes Wnt/β-catenin signaling in multiple myeloma by presenting Wnts and R-spondins. *Blood* 131: 982 – 994

Roderiquez G, Oravecz T, Yanagishita M, Bou-Habib DC, Mostowski H, Norcross MA (1995) Mediation of human immunodeficiency virus type 1 binding by interaction of cell surface heparan sulfate proteoglycans with the V3 region of envelope gp120-gp41. *J Virol* 69: 2233 – 2239

Sarrami-Forooshani R, Mesman AW, van Teijlingen NH, Sprokholt JK, van der Vlist M, Ribeiro CM, Geijtenbeek TB (2014) Human immature Langerhans cells restrict CXCR4-using HIV-1 transmission. *Retrovirology* 11: 52

Sungnak W, Huang NI, Bécavin C, Berg M, Queen R, Litvinukova M, Talavera-López C, Maatz H, Reichart D, Sampaziotis F *et al* (2020) SARS-CoV-2 entry factors are highly expressed in nasal epithelial cells together with innate immune genes. *Nat Med* 26: 681 – 687

Teng YH, Aquino RS, Park PW (2012) Molecular functions of syndecan-1 in disease. *Matrix Biol* 31: 3 – 16

Tsang NNY, So HC, Ng KY, Cowling BJ, Leung GM, Ip DKM (2021) Diagnostic performance of different sampling approaches for SARS-CoV-2 RT-PCR testing: a systematic review and meta-analysis. *Lancet Infect Dis* 21: 1233 – 1245

Vanders RL, Hsu A, Gibson PG, Murphy VE, Wark PAB (2019) Nasal epithelial cells to assess in vitro immune responses to respiratory virus infection in pregnant women with asthma. *Respir Res* 20: 259

Wang H, Liu Q, Hu J, Zhou M, Yu M-Q, Li K-Y, Xu D, Xiao Y, Yang J-Y, Lu Y-J *et al* (2020) Nasopharyngeal swabs are more sensitive than oropharyngeal swabs for COVID-19 diagnosis and monitoring the SARS-CoV-2 load. *Front Med (Lausanne)* 7: 334

Wang N, Shi X, Jiang L, Zhang S, Wang D, Tong P, Guo D, Fu L, Cui YE, Liu XI *et al* (2013) Structure of MERS-CoV spike receptor-binding domain complexed with human receptor DPP4. *Cell Res* 23: 986 – 993

Wang P, Nair MS, Liu L, Iketani S, Luo Y, Guo Y, Wang M, Yu J, Zhang B, Kwong PD *et al* (2021) Antibody resistance of SARS-CoV-2 variants B.1.351 and B.1.1.7. *Nature* 593: 130 – 135

de Witte L, Bobardt M, Chatterji U, Degeest G, David G, Geijtenbeek TB, Gallay P (2007a) Syndecan-3 is a dendritic cell-specific attachment receptor for HIV-1. *Proc Natl Acad Sci USA* 104: 19464 – 19469

de Witte L, Nabatov A, Pion M, Fluitsma D, de Jong MA, de Gruijl T, Piguet V, van Kooyk Y, Geijtenbeek TB (2007b) Langerin is a natural barrier to HIV-1 transmission by Langerhans cells. *Nat Med* 13: 367 – 371

World Health Organization (2020a) *Clinical management of COVID-19. Interim guidance 27 May 2020*, p. 62. Geneva: WHO Press – World Health Organization

World Health Organization (2020b) *Timeline of WHO's response to COVID-19*.

Wright L, Steptoe A, Fancourt D (2020) Are we all in this together? Longitudinal assessment of cumulative adversities by socioeconomic position in the first 3 weeks of lockdown in the UK. *J Epidemiol Community Health* 74: 683 – 688

Xia S, Liu M, Wang C, Xu W, Lan Q, Feng S, Qi F, Bao L, Du L, Liu S *et al* (2020) Inhibition of SARS-CoV-2 (previously 2019-nCoV) infection by a highly potent pan-coronavirus fusion inhibitor targeting its spike protein that harbors a high capacity to mediate membrane fusion. *Cell Res* 30: 343 – 355

Yuki K, Fujiogi M, Koutsogiannaki S (2020) COVID-19 pathophysiology: a review. *Clin Immunol* 215: 108427

Zhai Z, Li C, Chen Y, Gerotziafas G, Zhang Z, Wan J, Liu P, Elalamy I, Wang C (2020) Prevention and treatment of venous thromboembolism associated with coronavirus disease 2019 infection: a consensus statement before guidelines. *Thromb Haemost* 120: 937 – 948

Zhang QI, Chen CZ, Swaroop M, Xu M, Wang L, Lee J, Wang AQ, Pradhan M, Hagen N, Chen LU *et al* (2020) Heparan sulfate assists SARS-CoV-2 in cell entry and can be targeted by approved drugs in vitro. *Cell Discov* 6: 80

Zhang Z, Coomans C, David G (2001) Membrane heparan sulfate proteoglycan-supported FGF2-FGFR1 signaling: evidence in support of the "cooperative end structures" model. *J Biol Chem* 276: 41921 – 41929

Zhou P, Yang X-L, Wang X-G, Hu B, Zhang L, Zhang W, Si H-R, Zhu Y, Li B, Huang C-L *et al* (2020) A pneumonia outbreak associated with a new coronavirus of probable bat origin. *Nature* 579: 270 – 273

Zhu NA, Zhang D, Wang W, Li X, Yang BO, Song J, Zhao X, Huang B, Shi W, Lu R *et al* (2020) A novel coronavirus from patients with pneumonia in China, 2019. *N Engl J Med* 382: 727 – 733

Zou L, Ruan F, Huang M, Liang L, Huang H, Hong Z, Yu J, Kang M, Song Y, Xia J *et al* (2020a) SARS-CoV-2 viral load in upper respiratory specimens of infected patients. *N Engl J Med* 382: 1177 – 1179

Zou X, Chen K, Zou J, Han P, Hao J, Han Z (2020b) Single-cell RNA-seq data analysis on the receptor ACE2 expression reveals the potential risk of different human organs vulnerable to 2019-nCoV infection. *Front Med* 14: 185 – 192